Femtosecond laser structuring of graphite anodes for improved lithium-ion batteries: Ablation characteristics and process design

Cite as: J. Laser Appl. **30**, 032205 (2018); https://doi.org/10.2351/1.5040611
Submitted: 18 May 2018 . Accepted: 18 May 2018 . Published Online: 14 June 2018

Jan B. Habedank, Joseph Endres, Patrick Schmitz, Michael F. Zaeh, and Heinz P. Huber

Femtosecond laser structuring of graphite anodes for improved lithium-ion batteries: Ablation characteristics and process design

Jan B. Habedank,[1] Joseph Endres,[1] Patrick Schmitz,[1] Michael F. Zaeh,[1] and Heinz P. Huber[2]
[1]*Technical University of Munich, 85748 Garching, Germany*
[2]*University of Applied Sciences Munich, 80335 Munich, Germany*

(Received 18 May 2018; accepted for publication 18 May 2018; published 14 June 2018)

Lithium-ion batteries are widely used as energy storage devices due to their high energy density and versatile applicability. Key components of lithium-ion batteries are electrically isolated electrodes and a liquid electrolyte solution which enables ion transport between the electrodes. Laser structuring of electrodes is a promising approach to enhance the high-current capability of lithium-ion batteries by reducing cell internal resistances, as a larger contact area of the active material with the electrolyte solution is created. In the work described here, lithium-ion battery anodes were structured by locally ablating small fractions of the coating using femtosecond laser pulses with infrared wavelengths. A study on ablation characteristics depending on different process parameters such as laser fluence and repetition rate was performed. Special focus was on the ablation efficiency, enabling an optimized process design. The influence of the electrode composition was taken into account by studying the ablation behavior at a varying binder content. Evenly distributed micro holes were chosen in order to keep active material removal at a minimum. To evaluate the effect of structured graphite anodes on the electrochemical properties of lithium-ion batteries, test cells were manufactured and galvanostatically cycled at different current rates. Results show improvements in high-current performance which is expressed by an increased discharge capacity yield. © *2018 Laser Institute of America*. https://doi.org/10.2351/1.5040611

Key words: laser structuring, electrodes, lithium-ion batteries, graphite

I. INTRODUCTION

Lithium-ion batteries are currently the dominant energy storage solution for consumer electronics and electric vehicles. Rapid developments in material science and engineering have led to significant gains in performance, reliability, and safety of battery-powered products at shrinking costs.[1] In order to meet future customer expectations in automotive applications, the energy content per battery volume and mass as well as power delivery have to be increased. These conflicting requirements are greatly influenced by the electrode attributes. The electrodes typically consist of a composite layer made of active material, binder, and conductive agents coated onto metallic current collector foils.[2] As only the electrochemically active materials contribute to the deployable capacity of a cell, the content of non-active material per areal dimension has to be reduced. This can be achieved by decreasing the content of binder and conductive agent, increasing the compression of the porous material matrix, or raising the coating thickness.[3] Electrodes with a higher coating thickness contain more energy; therefore, fewer electrodes are required to reach the nominal cell capacity. However, such electrodes with high active material loading struggle with an increased cell resistance in operation, leading to performance losses at higher charge and discharge currents. The resistance is mainly caused by a limited transport speed of the ions through the porous electrode layer and results in an early meeting of voltage limits, amplified heat generation, and faster initiation of degradation processes.[4] It has been demonstrated that structured electrodes can have a positive impact on cell performance at higher current rates.[5–8] Simulative and experimental approaches attribute this to an increase of reaction surface and reduced diffusion pathways through the tortuous electrode structure, facilitating ion transport.

Femtosecond laser processing has been widely introduced as a precise and flexible patterning method with a negligible thermal damage zone.[9,10] Laser structuring of electrodes is currently not used in industrial production of lithium-ion batteries. However, several research studies have been published on this matter. Pröll *et al.*,[11] Smyrek *et al.*,[12] and Mangang *et al.*[13] focused on cathode materials and were able to observe a notable increase in deployable mass-specific capacity at high-current rates. They used different pulsed laser sources with pulse durations in the range from nanoseconds (ns) to femtoseconds (fs). When treating porous cathode materials such as lithium-nickel-manganese-cobalt-oxide (NMC), they created grid or channel structures that were filled with electrolyte during cell assembly. Pfleging *et al.* were able to observe improvements in the electrolyte wetting time as the electrolyte liquid is soaked in more rapidly by capillary forces.[14] Lutey *et al.* performed a study on the ablation of different electrode coatings including graphite with nanosecond laser pulses and analyzed the incision depths at different translational velocities.[15] Schmieder developed an analytical model of laser ablation mechanisms with ns laser pulses.[16] The study focused on the cutting

process of electrodes, limiting the transferability of the results for structuring. Hoffman *et al.* studied the effect of the laser wavelength and fluence on the ablation of solid carbon surfaces.[17] To our knowledge, neither the effect of laser structuring of graphite anodes on the battery performance nor the ablation characteristics of porous graphite anodes with femtosecond laser radiation have been thoroughly analyzed yet. However, the structuring of graphite anodes should have a high potential, as graphite particles usually have a flake-like shape and tend to arrange in a parallel manner to the substrate foils due to production processes, creating particularly long and branched ion migration paths.[18] This behavior is displayed in Fig. 1 (top).

By creating laser induced pores, the effective lengths of the ion migration paths are reduced and thereby the internal cell resistance is decreased. Simulations indicate that the increase in cell performance by reduced cell resistance strongly depends on the structure dimensions. Nemani *et al.* identified an aspect ratio >1 (relation between structure diameter and depth) to be of high importance, suggesting structures with small diameters and large structure depths.[19] As state-of-the-art electrodes usually have coating thicknesses of 50–100 μm, the desired structure diameters are <50 μm with a structure depth of >50 μm. To achieve these dimensions, mechanical manufacturing processes are unsuitable, especially as a large number of structures have to be created in a short amount of time. Laser structuring appears to be highly suitable for the manufacturing of the desired structure dimensions.

II. OBJECTIVES AND APPROACH

As described above, laser structuring of graphite anodes is expected to have a great potential for improving the performance characteristics of lithium-ion batteries by shortening ion migration paths. In this work, a study regarding the ablation characteristics of the porous coating material of the electrode is presented. Several laser parameters such as peak fluence and pulse frequency as well as different electrode compositions were taken into account. A special focus was put on the ablation efficiency, as high ablation rates will be necessary for industrial electrode production. Test cells were manufactured to demonstrate the benefit of laser structuring of graphite anodes as well as to rule out any potential damage to the electrochemically active components.

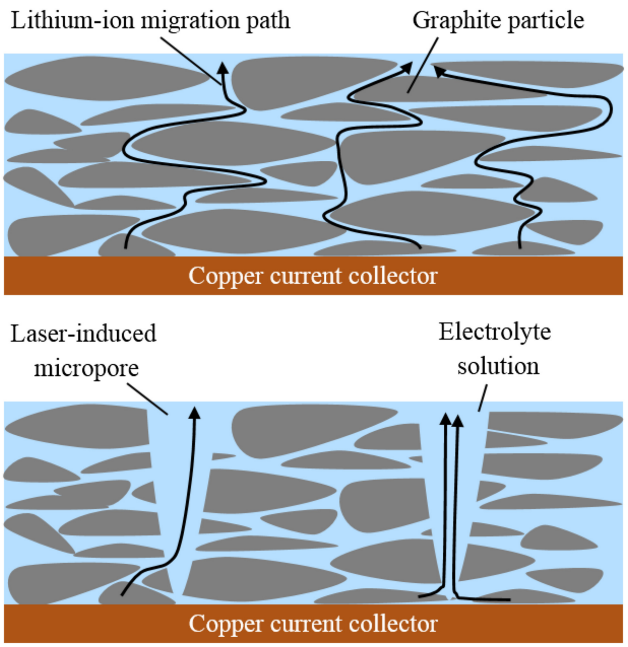

FIG. 1. Illustration of the lithium-ion flow through a graphite anode, top: unstructured electrode with long ion migration paths, bottom: structured electrode with short and direct ion migration paths.

III. MATERIALS AND METHODS

A. Electrode materials and fabrication

To ensure a high degree of comparability between separate ablation measurements, commercially available anodes with excellent homogeneity were chosen for the experiments. The material composition of the anodes was 92.5 wt. % graphite, 7.0 wt. % binder, and 0.5 wt. % conductive carbon coated onto both sides of a copper foil with a thickness of 10 μm. The coating thickness was 50 μm on both sides with a porosity of approximately 32%, resulting in a weight loading of 6.5 mg/cm^2 on each side. Other electrode characteristics as well as utilized production processes are unknown to the authors. For the studies on the ablation mechanisms with varying binder content as well as the production of test cells, tailored electrodes were manufactured. The anode ink was prepared by mixing 95.0 wt. % graphite (SGL Carbon) and 5.0 wt. % polyvinylidene fluoride (PVDF) with *N*-methyl-2-pyrrolidone (NMP, Sigma Aldrich) in a multi-step mixing process described in Günther *et al.*[20] The cathode ink contained 96.0 wt. % NMC (BASF), 2.0 wt. % PVDF, and 2.0 wt. % Carbon (C65, Timical). Mixing was performed in a planetary centrifugal vacuum mixer (Thinky ARV-310). Both inks were coated onto current collectors (anode: copper, cathode: aluminum) in a tape casting process and dried overnight at 50 °C to remove the NMP from the coating. After drying, the electrodes were compressed to a porosity of 35%. The resulting coating thickness after compression was 64 μm on average. Further details on the manufacturing process of electrodes can be found in Marks *et al.*[21]

B. Laser structuring and structure measurement

Laser structuring was performed using a pulsed femtosecond laser (Spirit® One™ 1040-8, Spectra-Physics) with a pulse duration τ_p of 400 fs and a wavelength λ of 1040 nm in ambient air. Specifications of the laser source such as the beam quality factor M^2 and the pulse energy E_p are presented in Table I.

TABLE I. Specifications of the laser source Spirit® One 1040-8.

λ (nm)	M^2	d_0 (μm)	τ_p (fs)	f_R (Hz)	E_p (μJ)
1040	1.2	17.2	400	10–10^4	max. 40

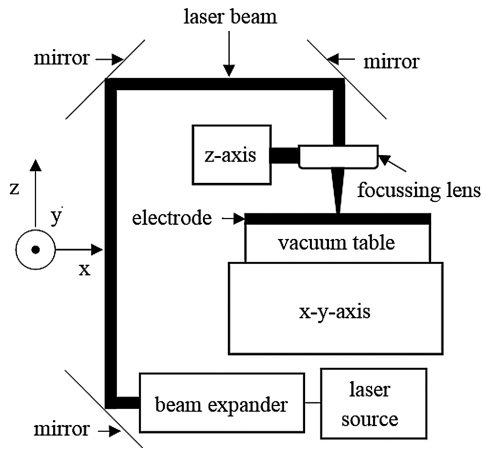

FIG. 2. Experimental setup for laser structuring of anodes.

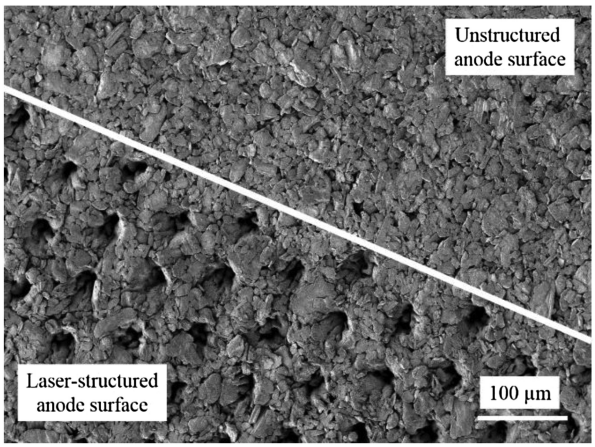

FIG. 3. Scanning electron microscopy image of a laser structured and an unstructured graphite anode surface.

The experimental setup is displayed in Fig. 2. The electrode was fixed using a vacuum clamping plate and moved in the *x*–*y*-plane in order to spatially distribute the structures. The laser beam was expanded before being focused on the electrode surface in order to achieve a small focus diameter.

The dimensions of the structures were measured using a confocal microscope (Leitz Ergoplan) and analyzed with the corresponding evaluation software (Gwyddion).

C. Cell assembly and testing

Coin cells were assembled in an argon filled glove box (M-Braun) with $H_2O < 0.1$ ppm and $O_2 < 0.1$ ppm. Prior to transferring the electrodes into the glovebox, they were dried overnight at 120 °C in a vacuum oven. All other cell components were dried overnight at 70 °C under vacuum. Two cell types were manufactured: reference cells with unstructured anodes and cells with structured anodes. The cathodes in all cells remained unstructured. Three cells of each type were produced to ensure statistical relevance. Cathode coins were 14 mm in diameter, anode coins 15 mm, and the glass microfiber separator (VWR, Type 691) 16 mm to ensure complete coverage of the cathode by the anode material and to avoid internal short circuits. Electrodes were matched to an area specific capacity ratio between anode and cathode of around 1.2 to 1. The electrolyte was LP572 (BASF) which consists of ethylene carbonate and ethyl-methyl-carbonate 3:7 with 1M lithium-hexafluorophosphate ($LiPF_6$) conductive salt and 2% vinylene carbonate.

After assembly, the cells went through formation by charging and discharging them three times at C/10 in a laboratory battery testing system (Basytec). The discharge capacity of the third cycle was defined as the theoretical capacity of the cell. To determine the rate capability, the cells were cycled from 4.2 to 3 V at increasing C-rates from C/10 to 5 C. Charging was done using a constant current constant voltage procedure with a charging current of C/10 for the corresponding discharge cycles with C/10, C/5, and C/2 and a charging current of C/2 for the corresponding discharge cycles with 1 C, 2 C, and 3 C. Discharging was performed using a constant current procedure.

IV. LASER ABLATION OF GRAPHITE ANODES

Separate holes with a distance of 70 μm and a structure diameter of approximately 25 μm were created and evenly distributed in a triangular pattern. However, due to the porous character of the electrode coating consisting of particles with different particle sizes, certain deviations in structure dimensions were observed. In contrast to line or grid structures, the hole pattern causes a large increase in electrode surface area while keeping the removal of active material at a minimum. An exemplary structure is displayed in Fig. 3 together with an image of the unstructured anode surface.

A. Peak fluence and number of repetitions

In order to evaluate the effect of the peak fluence

$$\Phi_0 = \frac{2 \cdot E_p}{r_0^2 \cdot \pi}, \tag{1}$$

and the number of applied pulses on the depth of the ablation craters, an analysis on ablation characteristics was performed. E_p is the pulse energy and r_0 is the radius of the laser beam in the focal plane. According to Nolte *et al.*, the ablation depth D can be described by Eq. (2), with the threshold fluence Φ_{th} and a scaling parameter δ:[22]

$$D = \delta^* \ln\left(\frac{\Phi_0}{\Phi_{th}}\right). \tag{2}$$

The experimental results are displayed in Fig. 4.

For each constant number of laser pulses, an increasing ablation depth D was observed when the peak fluence was increased. Also, a greater number of laser pulses with the same peak fluence led to an increased ablation depth. The parameters for the fit functions are presented in Table II. The fits were created using the least squares method.

However, a disproportionally large number of laser pulses n were needed to achieve a comparable ablation depth when the peak fluence was slightly decreased. This effect is

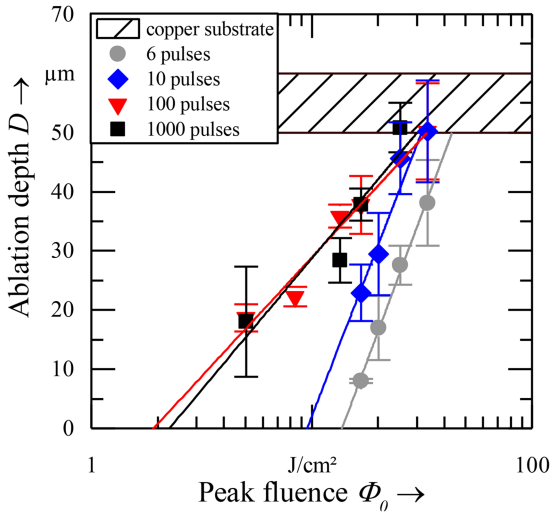

FIG. 4. Depths of ablation craters in graphite anodes for a varying number of applied pulses, standard deviations are displayed, $f_r = 10$ Hz, fits according to Table II.

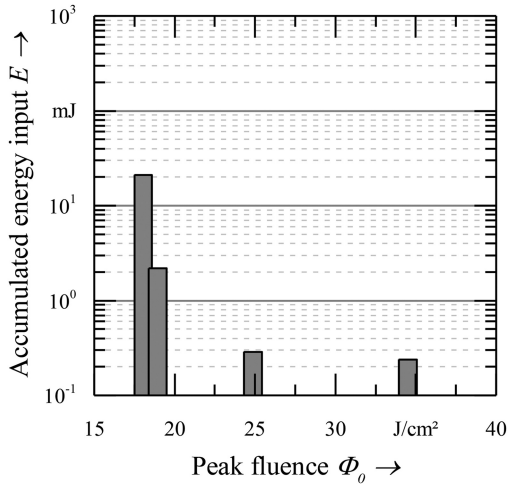

FIG. 5. Accumulated energy input E for a constant ablation depth of 40 μm into the graphite coating, $f_r = 10$ Hz.

presented in Fig. 5. The higher accumulated energy E that is introduced into the workpiece

$$E = n \cdot E_p = \frac{n \cdot \Phi_0 \cdot \pi \cdot r_0^2}{2}, \tag{3}$$

is an indication of the more inefficient ablation with smaller fluences.

The experiments were conducted with a pulse frequency of 10 Hz, in order to rule out effects that may occur due to heat accumulation, shielding by ablation products, or any other interaction between separate pulses. As the coating thickness of the electrode was approximately 50 μm, deeper penetration of the specimen could only be obtained by ablating a fraction of the copper current collector. This effect was not examined in further considerations.

It can be concluded that the single pulse fluence has a greater influence on the ablation depth than the accumulated energy that is introduced into the electrode over time. In order to accomplish a better process efficiency and short process times, large pulse fluences are essential. It has to be noted that even with the highest fluence applied, several pulses on the same spot were necessary to achieve significant structure depths >50% of the coating thickness. This brings up the question whether these pulses should be applied consecutively (forming one structure at a time) or in separate runs (structuring a certain electrode area repetitively). This issue is addressed in Sect. IV B.

TABLE II. Results for the logarithmic fits [Eq. (2)] displayed in Fig. 4.

Number of pulses (n)	δ (μm)	Φ_{th} (J/cm^2)
6	43.50	13.74
10	41.81	9.54
100	17.49	1.92
1000	19.31	2.26

B. Pulse fluence and repetition rate

For process design, it is crucial to evaluate the effects of an increasing pulse repetition rate on the process efficiency, especially as available industrial laser sources have been continuously gaining average power over the last years. Therefore, the influence of the pulse frequency at a varying peak fluence was determined. The number of applied pulses was 10 for all runs. The results are displayed in Fig. 6.

It becomes apparent that the pulse repetition rate has a significant influence on the amount of ablated material if all other process parameters remain constant. At low repetition rates (10 and 100 Hz), the influence of the repetition rate on the ablation depth was rather small. However, at higher rates,

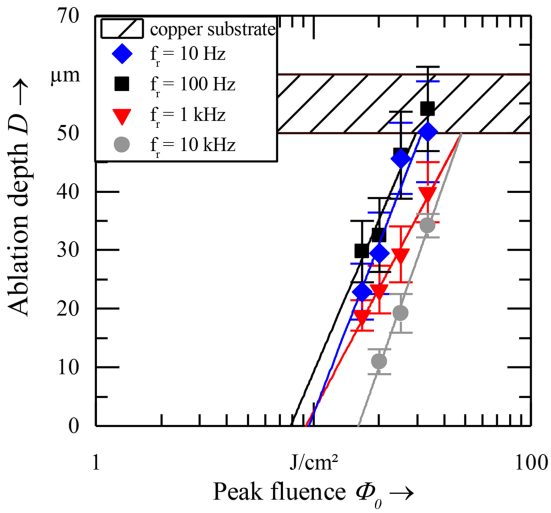

FIG. 6. Depths of ablation craters in graphite anodes for different pulse repetition rates, standard deviations are displayed, 10 pulses for all runs, fit according to Table III.

TABLE III. Results for the logarithmic fits [Eq. (2)] displayed in Fig. 6.

Repetition rate (f_r)	δ (μm)	Φ_{th} (J/cm^2)
10 Hz	41.81	9.54
100 Hz	37.63	7.86
1 kHz	30.33	9.25
10 kHz	45.74	16.11

the resulting ablation depth decreased significantly in case the pulses were applied on the same surface area. This may be attributed to heat accumulation or shielding effects caused by ablated graphite particles.

The parameters for the fit functions are presented in Table III. The fits were created using the least squares method.

In Fig. 7, the resulting structure depths are presented for different repetition rates from 10 Hz to 10 kHz. The peak fluence and the number of pulses were constant. If the structures were created one by one, a rise in repetition rate caused substantial losses in process efficiency. For a repetition rate of 10 kHz, an ablation depth of only 20 μm was observed, while at repetition rates <100 Hz, the ablation depth was approximately 45 μm, even though the energy input was identical.

As repetition rates below 100 Hz are much too slow for industrially relevant processes and at the same time large repetition rates cause laser ablation efficiency losses if structures are formed one at a time, the structures will have to be created in consecutive runs over a certain machining area. Thus, shielding effects can be avoided and the high pulse repetition rates of state-of-the-art laser sources combined with highly dynamic scanning optics can be exploited.

C. Influence of electrode composition on ablation

Additionally to the studies on the laser beam parameters such as peak fluence and repetition rate, an analysis of the influence of the electrode composition was carried out. Electrodes with a different content of PVDF binder were manufactured and laser structured with 10 laser pulses with a peak fluence of 33 J/cm^2 at a repetition rate of 1 kHz. The examined values of binder content were 2.0 wt. %, 5.0 wt. %, and 8.0 wt. %. The results are presented in Fig. 8. The ablation depth decreased significantly with an increasing binder content of the electrode. At 2.0 wt. % binder content approximately 37 μm of active material coating were removed compared to 18 μm at 5.0 wt. % and 14 μm at 8.0 wt. %. This indicates that small changes in binder content may lead to large alterations in ablation behavior of electrode material.

As the binder creates cohesion among the graphite particles, this result is highly plausible. If laser structuring of electrodes will gain importance in future electrode production, special attention should be paid to possible reductions in binder content or alternate binder types which could make ablation of the coating more effective.

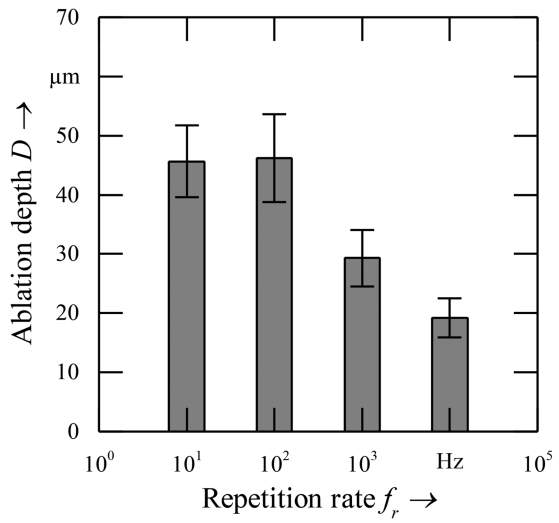

FIG. 7. Resulting ablation depths and standard deviations at different pulse repetition rates, 10 pulses per measurement point, $\Phi_0 = 25$ J/cm^2.

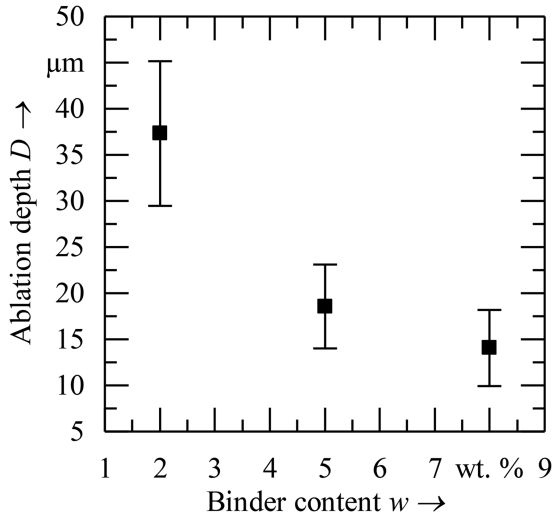

FIG. 8. Ablation depths and standard deviations of graphite anodes with a varying binder content, 10 pulses per measurement point, $\Phi_0 = 33$ J/cm^2, $f_r = 1$ kHz.

V. LI-ION CELLS WITH LASER STRUCTURED ANODES

To evaluate the beneficial effects of laser structuring of graphite anodes for lithium-ion batteries, test cells were manufactured. They were galvanostatically cycled at different C-rates from C/10 to 5 C. A C-rate of one represents a current that discharges the full capacity of a cell in one hour. The measured cell capacities at C/10 for the cells with unstructured anodes were 4.00, 3.69, and 3.90mAh. For structured anodes, the cell capacities were 4.00, 3.77, and 3.85 mAh, resulting in average capacities of 3.86 mAh for cells with unstructured anodes and 3.87 mAh with structured anodes. To facilitate a comparison between the cells, the discharge capacities were normalized with respect to the theoretical cell capacity. As the theoretical capacities of structured and unstructured cells and the electrode balancing are highly similar, this normalization is considered to not alter the results.

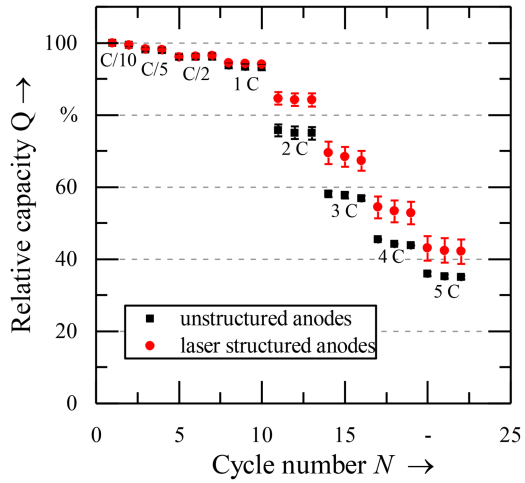

FIG. 9. Normalized discharge capacities and standard deviations of Li-ion coin cells with laser structured and unstructured anodes.

The results of the discharge rate test are presented in Fig. 9. The test indicated significant and substantial improvements in discharge capacity of approximately 20% for the cells with laser structured anodes compared to unstructured anodes for C-rates between 2 C and 5 C. At C-rates below 1 C, the reference cells and the cells with laser structured anodes showed almost equal performance. This indicates that no notable damage has been done to the surrounding active material particles by laser structuring, e.g., by creating a significant heat affected zone.

The improvements in the discharge characteristics of test cells with laser structured anodes can be attributed to reduced overpotentials and thereby decreased electrode polarization during discharge. The laser induced structures create lithium-ion migration paths that facilitate ion transport out of the electrode. In particular, the flake-like form of the graphite particles has repeatedly been suspected to slow down ion transport at high C-rates due to highly tortuous paths through the electrode's microstructure. This issue is partially overcome by laser structuring. It has to be noted that by laser structuring of anodes (in contrast to cathodes), the theoretical capacity of the cell is not decreased as the amount of active material on the cathode mainly determines the theoretical cell capacity. The active material loading on the cathode side is not changed, so if functional balancing of the electrodes is maintained, no reduction in theoretical capacity is created. This is of great importance, as commercial lithium-ion cells are operated in various current regimes and a capacity trade-off at varying C-rates is not likely to be accepted by customers.

VI. SUMMARY AND OUTLOOK

In this work, anodes for lithium-ion batteries were structured using femtosecond laser pulses. A detailed study on ablation characteristics was performed. A high laser peak fluence was identified to be more important for an efficient ablation process than the accumulated energy input into the electrode over time. High pulse repetition rates on the same electrode area should be avoided in order to circumvent shielding from ablation products. Lithium-ion cells with laser structured anodes were manufactured and tested. They outperformed their unstructured counterparts in terms of high-current capability, delivering a 20% higher discharge capacity at current rates >1 C. At low current rates, no reduction in capacity was detected. This makes laser structuring of anodes highly interesting for all high-current applications of lithium-ion batteries. The laser process may also contribute to the introduction of ultra-high energy density cells with thick electrodes, as a satisfactory C-rate capability is likely to be maintained. The authors will continue to work on optimizing structure design by electrochemical simulations, on experimental validation and also on the process scale up to prove the adaptability of the laser structuring process for large format lithium-ion batteries.

ACKNOWLEDGEMENTS

This work was financially supported by the German Federal Ministry of Economic Affairs and Energy (BMWi) under Grant No. 03ET6103F (SurfaLIB).

[1]A. Sakti, J. J. Michalek, E. R. Fuchs, and J. F. Whitacre, "A techno-economic analysis and optimization of Li-ion batteries for light-duty passenger vehicle electrification," J. Power Sources **273**, 966–980 (2015).
[2]R. Korthauer, *Handbuch Lithium-Ionen-Batterien* (Springer Berlin Heidelberg, Berlin, Heidelberg, 2013).
[3]H. Zheng, J. Li, X. Song, G. Liu, and V. S. Battaglia, "A comprehensive understanding of electrode thickness effects on the electrochemical performances of Li-ion battery cathodes," Electrochim. Acta **71**, 258–265 (2012).
[4]K. G. Gallagher, S. E. Trask, C. Bauer, T. Woehrle, S. F. Lux, M. Tschech, P. Lamp, B. J. Polzin, S. Ha, B. Long, *et al.*, "Optimizing areal capacities through understanding the limitations of lithium-ion electrodes," J. Electrochem. Soc. **163**, A138 (2015).
[5]S. Ferrari, M. Loveridge, S. D. Beattie, M. Jahn, R. J. Dashwood, and R. Bhagat, "Latest advances in the manufacturing of 3D rechargeable lithium microbatteries," J. Power Sources **286**, 25–46 (2015).
[6]M. Roberts, P. Johns, J. Owen, D. Brandell, K. Edstrom, G. El Enany, C. Guery, D. Golodnitsky, M. Lacey, C. Lecoeur, *et al.*, "3D lithium ion batteries—from fundamentals to fabrication," J. Mater. Chem. **21**, 9876 (2011).
[7]J. W. Long, B. Dunn, D. R. Rolison, and H. S. White, "Three-dimensional battery architectures," Chem. Rev. **104**, 4463–4492 (2004).
[8]M. Osiak, H. Geaney, E. Armstrong, and C. O'Dwyer, "Structuring materials for lithium-ion batteries: Advancements in nanomaterial structure, composition, and defined assembly on cell performance," J. Mater. Chem. A **2**, 9433 (2014).
[9]B. N. Chichkov, C. Momma, S. Nolte, A. Tünnermann, "Femtosecond, picosecond and nanosecond laser ablation of solids," Appl. Phys. A **63**, 109 (1996).
[10]X. Liu, D. Du, and G. Mourou, "Laser ablation and micromachining with ultrashort laser pulses," IEEE J. Quantum Electron. **33**, 1706–1716 (1997).
[11]J. Pröll, H. Kim, A. Piqué, H. J. Seifert, and W. Pfleging, "Laser-printing and femtosecond-laser structuring of LiMn2O4 composite cathodes for Li-ion microbatteries," J. Power Sources **255**, 116–124 (2014).
[12]P. Smyrek, J. Pröll, J.-H. Rakebrandt, H. J. Seifert, and W. Pfleging, in *SPIE LASE*, edited by U. Klotzbach, K. Washio, C. B. Arnold (SPIE, 2015), p. 93511D.
[13]M. Mangang, J. Pröll, C. Tarde, H. J. Seifert, and W. Pfleging, in *SPIE LASE*, edited by U. Klotzbach, K. Washio, C. B. Arnold (SPIE, 2014), p. 89680M.
[14]W. Pfleging, R. Kohler, and J. Pröll, "Laser generated microstructures in tape cast electrodes for rapid electrolyte wetting: new technical approach for cost efficient battery manufacturing," in *SPIE LASE*, edited by U. Klotzbach, K. Washio, C. B. Arnold (SPIE, 2014), p. 89680B.

[15]A. H. A. Lutey, A. Fortunato, A. Ascari, S. Carmignato, and L. Orazi, in *ASME 2014 International Manufacturing Science and Engineering Conference Collocated with the JSME 2014 International Conference on Materials and Processing and the 42nd North American Manufacturing Research Conference, Detroit, MI, June 9–13, 2014* (ASME, 2014).
[16]B. Schmieder, in *SPIE LASE*, edited by U. Klotzbach, K. Washio, C. B. Arnold (SPIE, 2015), p. 93511C.
[17]J. Hoffman, J. Chrzanowska, S. Kucharski, T. Moscicki, I. N. Mihailescu, C. Ristoscu, and Z. Szymanski, "The effect of laser wavelength on the ablation rate of carbon," Appl. Phys. A **117**, 395–400 (2014).
[18]M. Ebner, D.-W. Chung, R. E. García, and V. Wood, "Tortuosity anisotropy in lithium-ion battery electrodes," Adv. Energy Mater. **4**, 1301278 (2014).
[19]V. P. Nemani, S. J. Harris, and K. C. Smith, "Design of bi-tortuous, anisotropic graphite anodes for fast ion-transport in Li-ion batteries," J. Electrochem. Soc. **162**, A1415 (2015).
[20]T. Günther, N. Billot, J. Schuster, J. Schnell, F. B. Spingler, and H. A. Gasteiger, "The manufacturing of electrodes: Key process for the future success of lithium-ion batteries," AMR **1140**, 304–311 (2016).
[21]T. Marks, S. Trussler, A. J. Smith, D. Xiong, and J. R. Dahn, "A guide to Li-ion coin-cell electrode making for academic researchers," J. Electrochem. Soc. **158**, A51 (2011).
[22]S. Nolte, C. Momma, H. Jacobs, A. Tünnermann, B. N. Chichkov, B. Wellegehausen, and H. Welling, "Ablation of metals by ultrashort laser pulses," J. Opt. Soc. Am. B **14**, 2716–2722 (1997).